Proceedings of the 5th International Symposium on Steel Science (ISSS 2017)
Nov. 13-16, 2017, Kyoto, Japan: The Iron and Steel Institute of Japan

Post-uniform elongation and tensile fracture of TWIP steels

Seon-Keun Oh, Young-Kook Lee*

Department of Materials Science and Engineering, Yonsei University, Yonsei-ro 50, Seodaemun-gu, Seoul, Republic of Korea

Abstract: The objective of the present study is to elucidate the complicated interrelationship between necking, post-uniform elongation (e_{pu}), strain rate sensitivity (SRS), fracture mechanism and Al concentration in Fe-18Mn-0.6C-xAl twinning-induced plasticity steels. The addition of Al increased e_{pu} and reduction ratios in dimension of the neck part of tensile specimens due to raised SRS. Both 0Al and 1.5Al steels showed dimple structures in entire fractured surfaces including middle and edge parts after tensile tests, regardless of Al concentration. TWIP steels were failed by ductile fracture mechanism due to the rapid formation and coalescence of micro-voids just after necking strain. The *"orange peel"* phenomenon was observed in the surface of both strained 0Al and 1.5Al TWIP steel specimens. This phenomenon is primarily caused by the strain gradient among the grains, which results from the difference between tensile axis and orientation of grains, and enhanced by planar slip, mechanical twinning, and high C concentration. Surface cracking occurred in severe orange peel or the decarburized layer of TWIP steels.

1. Introduction

High manganese twinning-induced plasticity (TWIP) steel has attracted much attention due to its remarkable combination of high tensile stress (UTS) (>800 MPa) and high uniform elongation (e_u) (>60%), which is caused primarily by mechanical twinning occurring during plastic deformation [1-4]. However, Al-free TWIP steel possesses inappreciable post-uniform elongation (e_{pu}) [5], which is related to hole expansion [6]. Nevertheless, until now there are few articles on the behaviors of necking and e_{pu} of TWIP steels and on their dependencies of Al concentration. In recent, some of present authors [3] reported that the extremely low e_{pu} of Al-free C-bearing TWIP steel is most likely due to its negative strain rate sensitivity (SRS) and that the increase of e_{pu} in Al-added TWIP steel is attributed to the improved SRS. e_{pu} shows a proportionality to SRS in many materials [12]. This analysis was based on the previous results that negative SRS occurs due to dynamic strain aging (DSA) in Al-free C-bearing TWIP steel [3, 7-11] and is improved by the addition of Al due to suppressed DSA [3, 7].

However, not only a mechanical aspect of SRS, but also metallographic studies are necessary for better understanding of the behaviors of necking and e_{pu} in both Al-free and bearing TWIP steels. Thus, the present study restarted from the definition of e_{pu};. Because e_{pu} is non-uniform elongation from necking to failure in a stress *vs.* strain curve, e_{pu} strongly depends on when and how a tensile specimen fails. Namely, e_{pu} must be closely related to necking and fracture mechanism. Considering the fracture behavior of TWIP steel, Al-free TWIP steel with negligible e_{pu} abruptly fails almost without necking of gauge part during tensile deformation. This appears to indicate that the TWIP steel undergoes brittle fracture at least at the moment of failure, despite large e_u. However, surprisingly the fracture surfaces of tensile specimens revealed many fine dimples, a feature of ductile fracture generally accompanied by necking and e_{pu}, regardless of chemical compositions and strain rate [3, 7, 8, 13-17]. In spite of this controvertible fracture behavior of TWIP steel, it was reported that the fracture of TWIP steel occurs in association with the nucleation and coalescence of voids simply based on the SEM images of fracture surfaces showing many fine dimples [3, 7, 14, 18-21].

In recent, Fabrègue *et al.* [19] conducted *in-situ* observation of void formation with strain by means of X-ray microtomography. They found that the void densities of both Al-free austenitic TWIP steel and 316L austenitic stainless steel were even lower than those of Al alloys with the same *fcc* crystal structure; this matches well with the previous result reported by Lorthios *et al.* [20]. However, 316L stainless steel possessed significant necking and high e_{pu}.

* Corresponding author. E-mail: yklee@yonsei.ac.kr, telephone: +82 2 2123 2831.

Accordingly, the fracture mechanisms of TWIP steels, even Al-free TWIP steel, are yet to be clear; as a result, it is more difficult to understand the variation of e_{pu} with the addition of Al. In addition, there is still neither quantitative analysis of necking nor a report on the relationship between fracture and Portevin–Le Chatelier (PLC) band observed in Al-free TWIP steel [8, 22]. Therefore, the objective of the present study is to investigate the behaviors of necking, e_{pu} and tensile fracture of TWIP steels with and without Al comprehensively and quantitatively in viewpoints of not only void formation but also PLC band propagation using various experimental techniques.

2. Experimental procedure

Fe-18Mn-0.6C-(0, 1.5)Al (wt.%) TWIP steels were made using a vacuum induction furnace. Hereafter, the TWIP steels are called 0Al and 1.5Al specimens according to their Al concentrations. After solution-treated at 1100 °C for 2 h, the ingots were hot-rolled to ~6-mm thick plates at temperatures from ~1000 °C to 900 °C, and then water-quenched to room temperature. After surface descaling, the hot-rolled plates were cold-rolled from ~4-mm to ~1.5-mm thick sheets.

Tensile tests were conducted for the following observations; necking, fracture surface, PLC band propagation, crack propagation and void formation. All tensile specimens were made by wire electric discharge machining along the rolling direction from the cold-rolled sheet. All tensile specimens were annealed at 1000 °C for 10 min under vacuum, and then water-quenched. The average grain sizes of annealed 0Al and 1.5Al specimens were evaluated including annealing twins by the linear intercept method [23] and turned out to be ~35 and 39 μm, respectively. The annealed tensile specimens were strained at room temperature primarily at an initial strain rate ($\dot{\varepsilon}$) of 1×10^{-3} s^{-1}. For the measurement of SRS, the annealed tensile specimens were deformed until failure with various $\dot{\varepsilon}$ values ranging from 1×10^{-2} s^{-1} to 1×10^{-4} s^{-1}. Microstructures of the fractured specimens after tensile tests were observed using a field-emission scanning-electron microscope (FE-SEM).

3. Results and discussion

3.1 *Relationship between post uniform elongation and strain rate sensitivity*

The addition of Al improved the degree of necking, reduction ratio in area, and e_{pu}, as shown in the below Table 1.

Table 1. Post uniform elongations, relative strain rate sensitivities, and reduction ratio of area between deformed region and the fractured region after tensile tests of 0Al and 1.5Al TWIP steels

Steel	Post uniform elongation, e_{pu} (%)	Relative strain rate sensitivity, m	Reduction ratio in area (%)
0Al	0.3	-0.0234	9.5
1.5Al	2.7	-0.0201	25.2

The relative SRS values ($m = d\ln UTS/d\ln\dot{\varepsilon}$) of both 0Al and 1.5Al specimens were evaluated using flow curves measured. Both TWIP steels exhibited negative SRS values, regardless of Al concentration, but the m value was slightly increased by the addition of Al. An increase in SRS value with Al concentration matches well with an increase in e_{pu} value with Al concentration, as expected. As mentioned above, the low e_{pu} value of TWIP steels is known to be caused by negative SRS [24, 25]. Fig. 1 shows that the e_{pu} values are exponentially increased with the SRS value in various alloys. The e_{pu} values of 0Al and 1.5Al TWIP steels are good agreement with the e_{pu}-m curve for various alloys. The e_{pu} and SRS values of Fe-30Mn-3Si-3Al TWIP steel (C-free TWIP steel) were higher than those of 0Al and 1.5Al TWIP steels (C-bearing TWIP steel) due to the low DSA effect of C-free TWIP steel [25]. Accordingly, the proportional relationship between the SRS value and the e_{pu} value was reconfirmed and it was realized that the addition of Al up to 1.5 wt.% increased e_{pu} and the reduction ratio in area due to the increased SRS value.

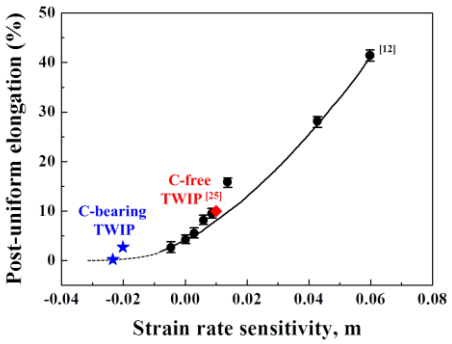

Fig. 1 Variation of post uniform elongation as a function of strain rate sensitivity in various alloys.

3.2 *Fracture mechanism*

The fractured surfaces of 0Al and 1.5Al specimens were observed after tensile tests using the SEM. All specimens showed dimple structures at the entire region including middle and edge parts (Figs. 2a and c), regardless of Al concentration, as reported previously by other researchers claiming ductile fracture [3, 7, 8, 13-17]. In addition, surface cracks were not observed in all fractured tensile specimens (Figs. 2b and d).

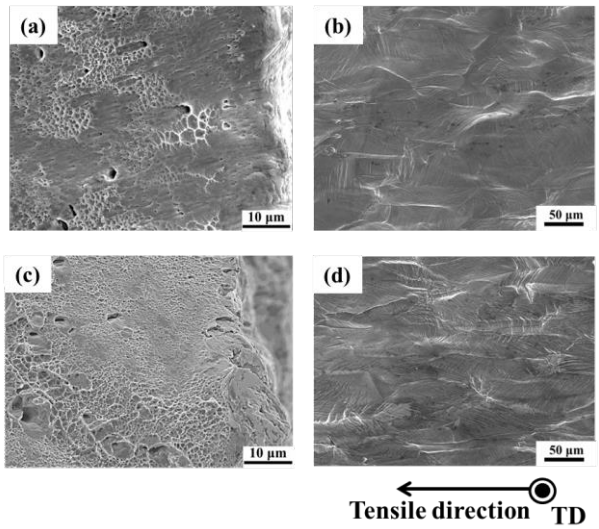

Fig. 2 Fractographs of the edge parts of fractured surfaces and SEM images of the side surfaces of fractured specimens; (a and b) 0Al and (c and d) 2Al specimens.

The ductile fracture is caused by the void nucleation and coalescence. The density and average size of micro-voids in Fe-22Mn-0.6C (wt.%) steel, measured by means of *in-situ* X-ray microtomography, were less than ~1000 mm^{-3} and ~4 μm at a necking strain [19]. Considering the fact that density and average size of micro-voids in Al alloys with the same *fcc* are ~60,000-80,000 mm^{-3} and ~5 μm at a necking strain [26], it is difficult to understand that the fracture mechanism of TWIP steel is ductile fracture due to a significantly low density of micro-voids of C-bearing TWIP steel. Fortunately, Lorthios *et al.*'s research [20] casts a hint of the fracture mechanism of TWIP steel. Lorthios *et al.* [20] reported that many fine micro-voids may form instantaneously at the last fracture stage in Fe-22Mn-0.6C (wt.%) steel. In addition, some large voids of several hundred microns were observed to be parallel to the fracture surface near the fracture tip. Based on the above results, micro-voids are inactively generated until the necking strain, and then abruptly nucleated and coalesced with further strain. Therefore, it is considered that TWIP steel exhibits ductile fractured surface although it shows little necking.

If the surface of TWIP steels is decarburized during heat treatment and ε-martensitic transformation occurs in the decarburized layer, the brittle fracture may arise at the surface of the TWIP steel. However, without decarburization, surface cracking was observed in Fe-14Mn-1.4C (wt.%) Hadfield steels due to severe inhomogeneous deformation between grains or due to carbide particles near the surface [15]. However, the exact cause has yet to be clarified, and further research is needed.

3.3 *Orange peel*

As mentioned in the previous section, surface cracks were not observed in tensile-fractured 0Al and 1.5Al specimens. However, the surfaces turned out to be rough after tensile tests, as shown in Fig. 3.

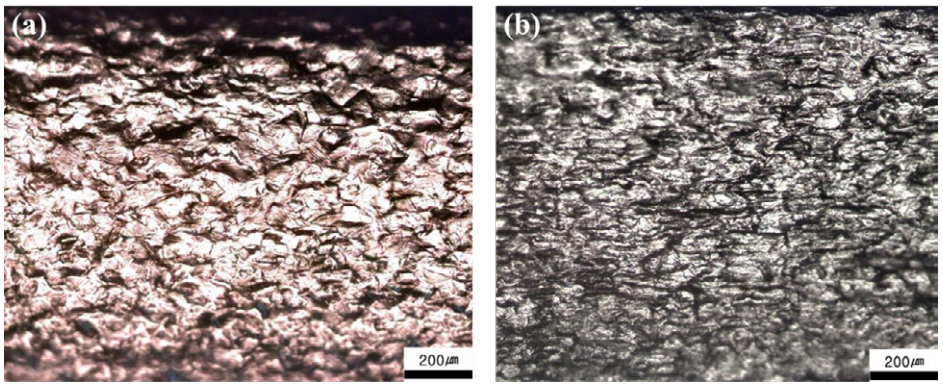

Fig. 3 Optical images of the side surfaces of (a) 0Al and (b) 1.5Al tensile specimens after tensile tests. The side surfaces were mirror-polished before tensile testing.

Although this rough surface has not been reported in TWIP steels, it was observed in a round-type tensile-fractured specimen of Fe-14Mn-1.4C (wt.%) Hadfield steel [15]. The surface of the specimen became rough like *"orange peel"*, and also revealed many cracks almost orthogonal to tensile direction. Rittle and Roman [27] reported that the *orange peel* phenomenon occurs when a single slip system is activated for deformation. Abbasi [15] explained that grain boundaries are crinkled because mechanical twining causes the reorientation of grains. In addition, inhomogeneous deformation occurs in the body of tensile specimen due to increasing reorientation of grains, resulting from micro twins generated inside each grain. Accordingly, the surfaces of grains that have free surface are rumpled similar to grain boundaries due to their lower strength and ductility.

However, the *orange peel* phenomenon was also observed at the side surfaces of tensile fractured 1.5Al TWIP steel (Fig. 3b) and carbon steel. Therefore, it was realized that the *orange peel* is not caused only by planar slip or mechanical twinning. Fundamentally, grains would not be deformed uniformly during the tensile test due to the difference between the tensile axis and the orientations of grains. Accordingly, *orange peel* is basically caused by the strain gradient among the grains resulting from the difference between the tensile axis and the orientations of grains, and can be enhanced by planar slip or mechanical twinning.

4. Conclusions

(1) The addition of Al up to 1.5 wt.% increased necking, e_{pu}, and the reduction ratio in area due to the improved SRS value.

(2) Both steels showed dimple structures in the entire fractured surfaces including middle and edge parts after tensile tests, regardless of Al concentration. Accordingly, it is thought that TWIP steels underwent ductile fracture with little necking due to the rapid nucleation and coalescence of micro-voids immediately after necking.

(3) Surface cracking occurs in the decarburized TWIP steel and high C Hadfield steels, resulting in the brittle-fractured surfaces.

(4) The *"orange peel"* phenomenon was observed in both 0Al and 1.5Al TWIP steels used in present study. This phenomenon is basically caused by strain gradient among the grains, resulting from

the difference between the tensile axis and the orientations of grains; it can be enhanced by planar slip or mechanical twinning.

REFERENCES

[1] O. Grässel, L. Krüger, G. Frommeyer, L.W. Meyer: Int. J. Plasticity, 16(10–11) (2000), 1391-1409.
[2] Y.-K. Lee: Scr. Mater., 66(12) (2012), 1002-1006.
[3] J.-E. Jin, Y.-K. Lee: Acta Mater., 60(4) (2012), 1680-1688.
[4] B.C. De Cooman, O. Kwon, K.G. Chin: Mater. Sci. Technol., 28(5) (2012), 513-527.
[5] I.-J. Park, S.-M. Lee, H.-H. Jeon, Y.-K. Lee: Corros. Sci., 93 (2015), 63-69.
[6] L. Chen, J.K. Kim, S.K. Kim, G.S. Kim, K.G. Chin, B. De Cooman: Steel Res. Int., 81(7) (2010), 552-568.
[7] H.K. Yang, Z.J. Zhang, F.Y. Dong, Q.Q. Duan, Z.F. Zhang: Mater. Sci. Eng. A, 607 (2014), 551-558.
[8] G. Scavino, F. D'Aiuto, P. Matteis, P. Russo Spena, D. Firrao: Metall. Mater. Trans. A, 41(6) (2010), 1493-1501.
[9] J.K. Kim, L. Chen, H.S. Kim, S.K. Kim, G.S. Kim, Y. Estrin, B. De Cooman: Steel Res. Int., 80(7) (2009), 493-498.
[10] A.K. Ghosh, R.A. Ayres: Metall. Mater. Trans. A, 7A (1976), 1589-1591.
[11] J.-K. Kim, L. Chen, H.-S. Kim, S.-K. Kim, Y. Estrin, B. De Cooman: Metall. Mater. Trans. A, 40(13) (2009), 3147-3158.
[12] A. Ghosh: J. Eng. Mater. Technol., 99(3) (1977), 264-274.
[13] A. Pineau, A.A. Benzerga: Acta Mater., 107 (2016), 424-483.
[14] Y.J. Dai, T. Di, Z. Mi, J. Lü: J. Iron Steel Res. Int., 17(9) (2010), 53-59.
[15] M. Abbasi, S. Kheirandish, Y. Kharrazi, J. Hejazi: Mater. Sci. Eng. A, 513-514 (2009) 72-76
[16] S. Kang, J.-G. Jung, M. Kang, W. Woo, Y.-K. Lee: Mater. Sci. Eng. A, 652 (2016), 212-220.
[17] S. Kang, Y.-S. Jung, J.-H. Jun, Y.-K. Lee: Mater. Sci. Eng. A, 527(3) (2010), 745-751.
[18] D. Fabrègue, C. Landron, O. Bouaziz, E. Maire: Steel Res. Int., 86(10) (2015), 1197-1203.
[19] D. Fabrègue, C. Landron, O. Bouaziz, E. Maire: Mater. Sci. Eng. A, 579 (2013), 92-98.
[20] J. Lorthios, F. Nguyen, A.F. Gourgues, T.F. Morgeneyer, P. Cugy: Scr. Mater., 63(12) (2010), 1220-1223.
[21] J. Lorthios, M. Mazière, X. Lemoine, P. Cugy, J. Besson, A.-F. Gourgues-Lorenzon: Int. J. Mech. Sci., 101-102 (2015), 99-113.
[22] J.G. Kim, S. Hong, N. Anjabin, B.H. Park, S.K. Kim, K.G. Chin, S. Lee, H.S. Kim: Mater. Sci. Eng. A, 633 (2015), 136-143.
[23] C.S. Smith, L. Guttman: Trans. Metall. Soc., AIME 197 (1953), 81-87.
[24] D.G. Ellwood: Mechanical metallurgy, New York, McGraw-Hill, 1961.
[25] H.K. Yang, Y.Z. Tian, Z.J. Zhang, Z.F. Zhang: Mater. Sci. Eng. A, 655 (2016), 251-255.
[26] E. Maire, S. Zhou, J. Adrien, M. Dimichial: Eng. Fract. Mech, 78 (2011) 2679-2690.
[27] D. Rittel, I. Roman: Metall. Mater. Trans. A, 19A (1988) 2269-2277